Journal of Water & Health

Journal of Water and Health Vol 21 No 6, 719 doi: 10.2166/wh.2023.303

Appraisal of surface–groundwater anthropogenic indicators and associated human health risk in El Sharqia Governorate, Egypt

Abdel Hameed M. El-Aassar[a], Rasha A. Hussien[b], Faten A. Mohamed[b], Selda Oterkus[c] and Erkan Oterkus[c,*]

[a] Egypt Desalination Research Center of Excellence (EDRC) and Hydrogeochemistry Department, Desert Research Center (DRC), Cairo, Egypt
[b] Nuclear and Radiological Safety Research Center, Egyptian Atomic Energy Authority (EAEA), Cairo, Egypt
[c] PeriDynamics Research Centre (PDRC), University of Strathclyde, Glasgow, United Kingdom
*Corresponding author. E-mail: erkan.oterkus@strath.ac.uk

ABSTRACT

The aim of this study was to integrate hydrogeochemistry with a multivariate statistical approach to understand the various processes that control the evolution/contamination of water resources in El Sharqia Governorate, Egypt with a particular emphasis on direct/indirect risks to human health. To achieve this, a representative collection of 21 groundwater and 35 drainage samples was taken and examined for physical, chemical, and trace element measurements. Results indicated that in shallow groundwater and drainage water samples, the relative abundance of major cations is $Na^{+} > Mg^{2+} > Ca^{2+} > K^{+}$, and for anions it is $HCO_3^{-} > Cl^{-} > SO_4^{2-}$ (on a molar basis). Natural processes involving the dissolution/precipitation of some minerals and other processes including leaching of solid waste, overuse of agricultural fertilizers application, and high loads of discharged sewage water are responsible for the evolution of water resources in El Sharqia Governorate. Ammonia, nitrate, biological oxygen demand (BOD), phosphate, turbidity, iron, manganese, lead, and aluminum concentrations were found to be higher than the limits set by internatio2nal drinking water regulations. The health risk index (HRI) values for children were found to be higher than those for adults when the water resources are used for drinking purposes, which poses a risk to human health.

Key words: Egypt, El Sharqia Governorate, geochemical modeling, human health risk, hydrochemistry, modeling mixing process

HIGHLIGHTS

- An integration of hydrogeochemistry with a multivariate statistical approach was applied.
- Various processes that control the evolution/contamination of water resources in El Sharqia Governorate, Egypt were investigated.
- A particular emphasis on direct/indirect risks to human health was given.
- A risk to human health was found.
- HRI values for children were higher than those for adults when used for drinking purposes.

GRAPHICAL ABSTRACT

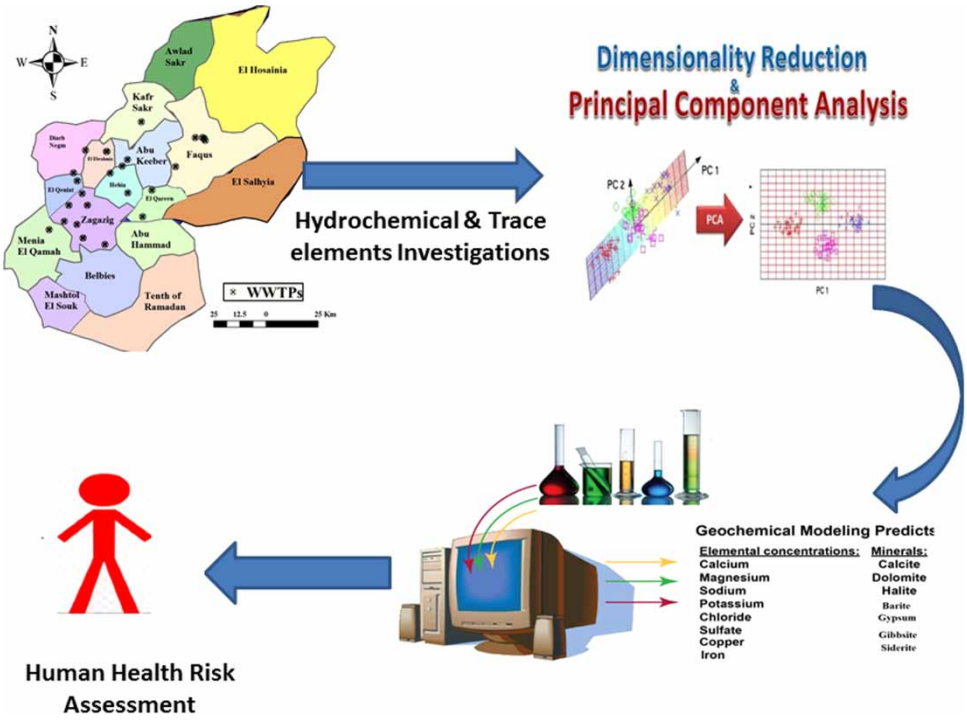

1. INTRODUCTION

Water is an essential part of our life; however, freshwater makes up a tiny portion of only 0.01% of the entire amount of water on the earth's surface (Amini *et al.* 2016; Moghaddama *et al.* 2018) and the vast bulk of the water on the earth's surface is saline or salt water (with an average salinity of 35%). Increasing human population, rapid urbanization rate, and industrial expansion led to an increment of water necessities all over the world, especially in developing countries. Water resources can be surfaces such as lakes, canals, or groundwater that are buried under the ground surface in geological formations (aquifers). In general, two main constraining factors defining water suitability for different agricultural, domestic, and industrial purposes are water availability or quantity and quality. Relying on surface water alone is not sufficient to meet these demands because of its limitations and inadequacy in most arid and semi-arid areas of developing countries. Consequently, reliance on groundwater resources has dramatically increased in these regions (Zhou *et al.* 2020). However, human activities have negative impacts on groundwater quality. Several anthropogenic pollution sources were found to be responsible for deterioration of water resources in developing countries such as industrial wastewater discharges, use of fertilizers and pesticides, wastewater irrigation, and atmospheric transportation that have led to the accumulation of heavy metals in the soils worldwide, especially in developing countries. The risks to human health caused by exposure to heavy metals present should not be disregarded in light of the aforementioned issues. It is crucial to assess the level of heavy metal pollution in soil and agricultural regions as well as the potential health risks caused by these toxicants. Non-point source pollution from discharging wastewater is the greatest threat to the sustainable use of water resources (surface and groundwater) in megacities. Excess untreated wastewater from villages and rural areas in the majority of developing countries is frequently discharged directly into water pathways, while household, commercial, and industrial effluents, as well as raw, untreated sewage are frequently dumped into surface and groundwater sources. Rainstorms eventually wash the wastewater into the water bodies or it percolates there. Stagnating wastewater in open lagoons and on the sides of the road frequently serves as a mosquito-breeding ground and a haven for various germs and viruses. Additionally, harmful substances like oil and grease, insecticides, ammonia, and heavy metals are present in wastewater pools. When point source pollution is reduced in many countries (even if wastewater treatment plants (WWTPs) begin to reach their capacity limits), climate (global) change impacts could increase pollution due to urban or agricultural run-off. In recent years, groundwater investigations were paying attention to assessing

and understanding the hydrochemical characteristics and water quality using several effective tools, including geochemical modeling, Geographical Information System (GIS), statistical approaches (multivariate statistical analysis), and water quality indices. Many factors control groundwater hydrochemistry including dissolution, precipitation, ion-exchange, sorption–desorption together with residence time along the flow path. A number of geochemical models were developed for tracing groundwater evolution along the flow path through inverse modeling or studying different mixing processes affecting the quality of water resources in the studied areas. The use of geochemical models is increasing in addressing groundwater quality problems involving geochemistry (Slimani *et al.* 2015; Berihu *et al.* 2017; Liu *et al.* 2020). Assessment of the contamination risk of water resources to human health is a useful technique for determining the potential negative consequences of environmental pollutants. This method has been used extensively to estimate the heavy metal contamination of drinking water and soils (Liu *et al.* 2016; Fakhri *et al.* 2018; Kamani *et al.* 2018; Keramati *et al.* 2018a, 2018b; Rezaei *et al.* 2018; Youssef *et al.* 2018). Recently, many studies have focused on this field (Sohrabi *et al.* 2016; Fakhri *et al.* 2018; Kamani *et al.* 2018; Keramati *et al.* 2018a, 2018b; Rezaei *et al.* 2018; Youssef *et al.* 2018) and this technique has been widely utilized to determine the level of heavy metal contamination of soils and drinking water (Liu *et al.* 2016, Fakhri *et al.* 2018). The main objectives of the present study is an integration of hydrochemical and multivariate statistical investigations to evaluate major and minor nutrients including chemical and trace elements measurements (ammonia, nitrate, phosphate, biological oxygen demand (BOD), chemical oxygen demand (COD), total organic carbon (TOC), oil, and grease) to identify anthropogenic indicators for surface and groundwater resources. There are also geochemical modeling applications, especially for mixing processes that affect the chemical composition and water quality of El Sharqia Governorate. Finally, we assess potential human health risk hazards of trace elements for different age groups of people including children and adults who probably rely on these water resources for different purposes.

2. STUDY AREA DESCRIPTION

The Governorate of El Sharqia under study is situated in the northern Nile Delta of Egypt, approximately between longitudes 31° 15′ and 32° 15′ E and latitudes 30° 20′ and 31° N with a 4,922 km^2 territory, it overtakes Al-Behaira Governorate as the second-largest governorate in the Nile delta region. According to the Egyptian Central Agency for Public Mobilization and Statistics, its population exceeded 7 million inhabitants per capita in 2017 and is projected to reach 10 million inhabitants per capita in 2032. The Eastern Delta region, Egypt, was taken as a pilot area that suffers from surface and groundwater deterioration due to excessive use of treated/untreated sewage effluent for irrigation purposes causing many human health hazards as shown in Figure 1(a). The study area is currently served by a sewerage system including integrated WWTPs as shown in Figure 1(b). The combined primary and secondary treated wastewater, with agricultural and industrial wastes, are discharged to some drainage channels combined with the untreated excess flow that is disposed of directly to the nearby main drains and then to Manzala Lake. Please note that drainage water in the study area implies streams that contain the excess of irrigated water seepage from the surrounding agricultural fields. Several studies on soil productivity potentials, hydrochemical and groundwater quality evaluation (Embaby *et al.* 2014; Mansour 2020), seasonal variations in the microbiological and physiochemical characteristics of municipal wastewater (Mahgoub *et al.* 2015), the effects of on-site sewage disposal on groundwater at Minia Al-Qamh, (Atwa *et al.* 2015), sedimentological and hydrochemical studies of groundwater (Mabrouk *et al.* 2016), hydrogeological investigations of the quaternary aquifer (El-Sayed *et al.* 2011), and soil productivity potentials (Rashed 2016) were all conducted in the El Sharqia Governorate. The values of ammonia, nitrate, BOD, phosphate, turbidity, iron, manganese, lead, and other contaminants were found to exceed the limits of drinking water international standards.

3. GEOLOGICAL AND HYDROLOGICAL SETTINGS

Deposits from the quaternary and tertiary acquifers make up the majority of the eastern Nile Delta as shown in Figure 2. The Nile sediments that occasionally have sands blown into them define the quaternary deposits. The sand, clay, and gravel content of the sediments vary both laterally and vertically. Uncomfortably, such sediments are present on the older units of Pleistocene tertiary. Early, Middle, and Late Pleistocene are used to categorize ancient deltaic deposits. Loose sands with cherty pebbles are a good representation of early Pleistocene deposits. They get thicker in the north, reaching a maximum thickness of roughly 900 m in El Matariya, and get thinner in the east. As a result, the deposits from the Middle Pleistocene are referred to as Mit Ghamr Formation. Sands and gravel with sporadic, discontinuous clay lenses serve as their

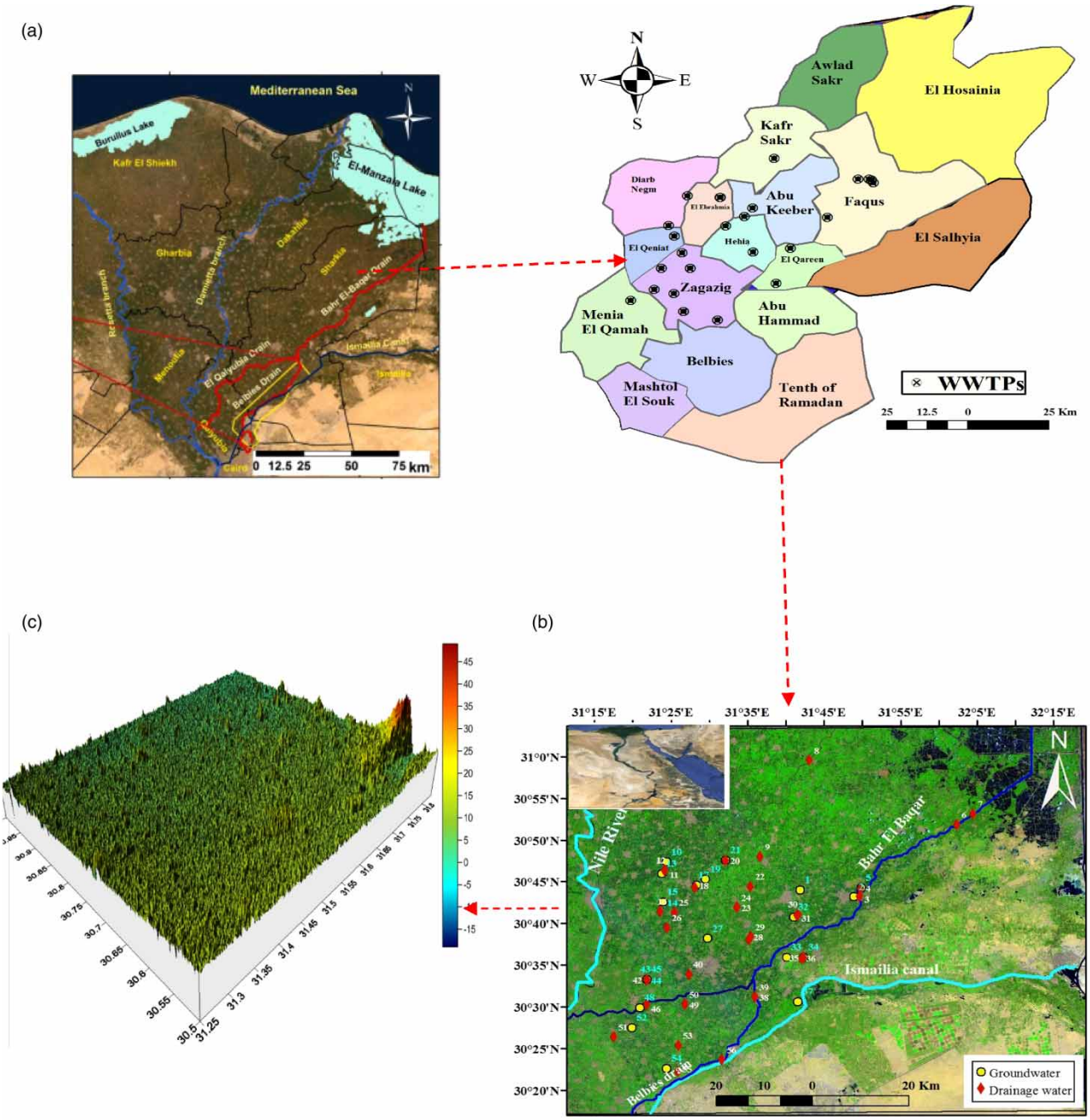

Figure 1 | (a) Map of the study area with drainage and groundwater sample locations; (b) location of WWTPs in El Sharqia Governorate; and (c) the digital elevation model (DEM).

representation. The sandy aquifer of the eastern Nile Delta is densely covered in erratic paleo-topography, including submerged Gizera sands and abandoned canals. Fluvial sediments serve as a representation of the top portions. Fluvial sediments form the higher portions. The Mit Ghamr formation in general and these sands, in particular, constitute significant parameters in the restriction of pollution of this aquifer. Sand and clay intercalations, in certain places covered by a thin, hard, crusty, sandy limestone deposit, define the Late Pleistocene.

As a result, clay was hydrogeologically partitioned from fluviatile deposits (river sands), fine to medium sands with thin intercalations of clay and silt, with a maximum thickness of around 30 m. This reflects the floodplain deposits of the former Damietta Branch. It symbolizes the upper, unconfined aquifer with intercalated clay. In the western regions, the

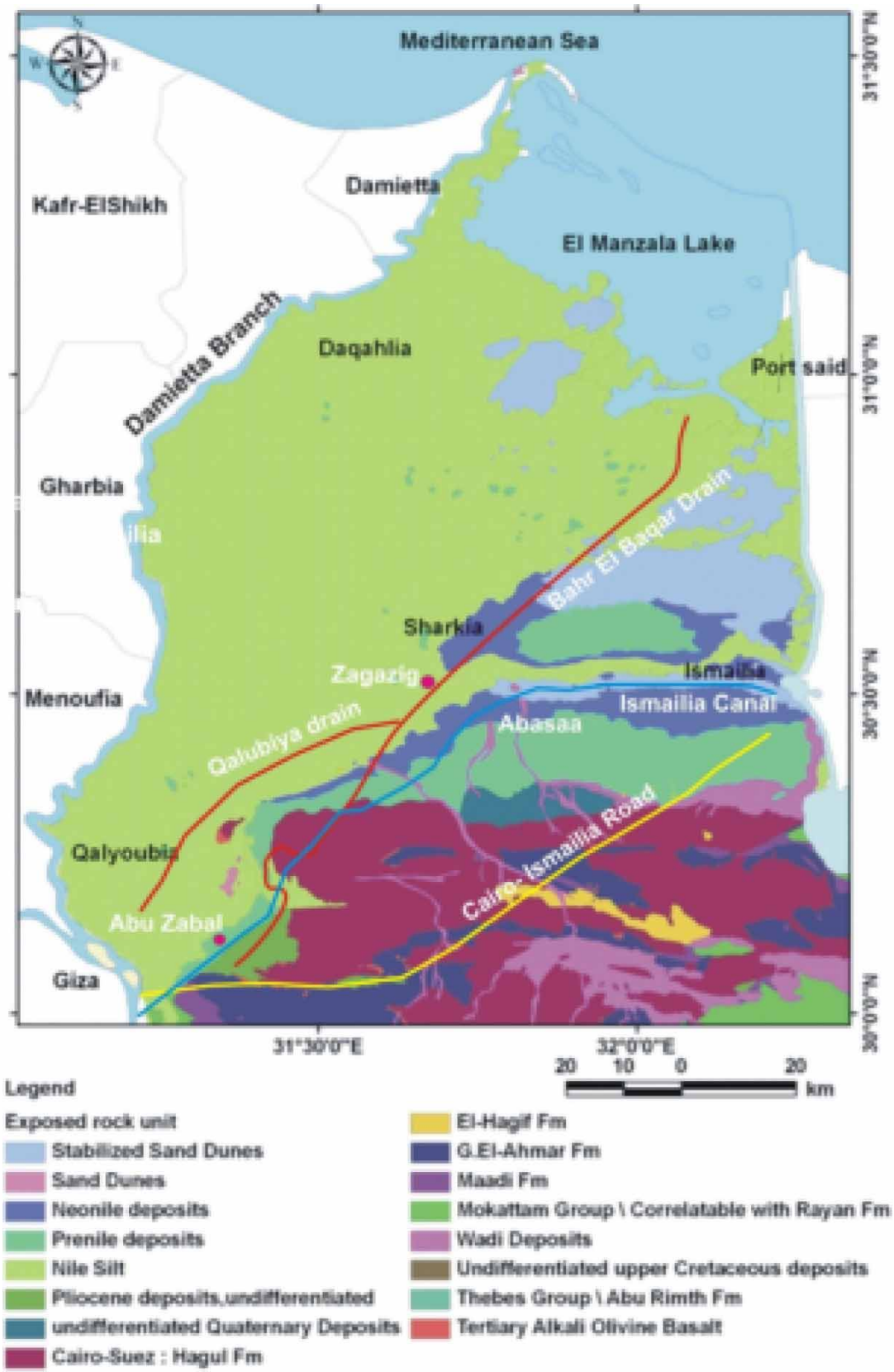

Figure 2 | Geological map of the study area.

ratio of sand to clay can exceed 50%, while it declines in the east and north. This series' alternation of coarse and fine particles supports the idea that these sediments date from the Late Pleistocene.

4. MATERIALS AND METHODS

4.1. Sample collection and analysis

Fieldwork was conducted in 2021 by collecting a representative set of 35 drainage and 21 groundwater samples. These water samples were collected in 500-mL pre-washed polyethylene bottles with de-ionized water. The samples were kept at 4 °C in the laboratory to prevent microbial changes in water chemistry. The samples were geo-referenced using GPS (Trimble, Juno S-3 model). Samples were analyzed at the hydrogeochemistry department of Desert Research Center (DRC) according to the methods adopted by the United States Geological Survey (Rainwater & Thatcher 1960; Fishman & Friedman 1989) and the American Society for Testing and Materials (ASTM 2002). The chosen wells have a depth range of 8–13 m below the surface. Major cation (Ca, Mg, Na, and K) and anion (Cl, SO_4, and HCO_3) concentrations were measured as chemical parameters. At the time of the sampling, all wells in El Sharqia Governorate were in operation (Figure 1). Using conventional EDTA, total hardness (TH) of $CaCO_3$ and Ca^{2+} was examined. Mg^{2+} was determined. A flame photometer was used to measure the levels of Na^+ and K^+. By titrating with HCl, the total alkalinity, $CaCO_3$, CO_3^{2-}, and HCO_3^- were calculated. Using the conventional Hg $(NO_3)_2$ titration, Cl was determined. A UV/Visible spectrophotometer was used to analyze SO_4^2 and NO_3. Trace element contents (Al^{3+}, Cd^{2+}, Cr^{3+}, Cu^+, Fe^{2+}, Mo^{2+}, Mn^{2+}, Ni^{2+}, Pb^{2+}, V^{5+}, and Zn^{2+}) of the water samples were determined using inductively coupled argon plasma (ICP). The obtained chemical data are expressed in milligrams per litre (mg/l) . Some parameters including the depth to water, total well depth, pH, temperature, EC, CO_3^{2-}, HCO_3^-, TOC, COD, and NO_3^- were determined *in situ* using pH, EC meter, 3510 Jenway – UK, for CO_3^{2-}, HCO_3^- titrimetrically against sulfuric acid by neutralization and measure of TOC, COD, and NO_3^- by using compact photometer PF-12Plus (Macherey–Nagel GmbH & Co. KG, filter photometer). The units of measurement for all parameters are mg/l and meq/l. The charge balance between the difference of cations and anions (expressed in meq/l) divided by their sum was used to evaluate the quality of the data:

$$\frac{\sum(\text{Cations} - \text{Anions})}{\sum(\text{Cations} + \text{Anions})} \times 100 \tag{1}$$

4.2. Geochemical modeling

In the domains of hydrogeology and geochemistry, the saturation index is a crucial geochemical statistic that is frequently helpful for determining the presence of several common minerals in the groundwater system (Deutsch 1997). The following equation (Lloyd & Heathcote 1985) was used in this investigation to determine saturation indices (SIs):

$$SI = \frac{\log(IAP)}{K_s(T)} \tag{2}$$

where K_s (T) is the equilibrium constant of the reaction taken into consideration at the sample temperature, and IAP is the relevant ion activity product, which may be computed by multiplying the ion activity coefficient I and the composition concentration mi. SI equals zero when the groundwater is fully saturated with certain minerals; positive SI values indicate oversaturation, and negative SI values indicate undersaturation (Appelo & Postma 1994; Drever 1997). The two or more end-members that participate in the mixing process inside the aquifer and contribute to recharge are identified using a simulation of the mixing process. Finally, the modeled composition of the mixture is compared to the actual composition of water found at the quaternary aquifer.

4.3. Human health risk assessment

The phrase 'exceedance level,' which refers to a unitless notion, is used to describe the extent to which various PTMs (potential toxic metals) exceed their respective World Health Organization (WHO) permitted limits and can be expressed as:

$$\text{Exceedance level} = \frac{\text{Concentration of a quality parameter}}{\text{WHO acceptable limit}} \tag{3}$$

In the studied area, both anthropogenic and natural factors contributed to the contamination of the majority of the groundwater. Additional analysis, including chronic daily intake (CDI) and health risk index (HRI) calculations, should be made to determine how much human health risk exposure is there (HRI). The consumption rate of element concentrations and the kind of toxicity are the key determinants of chronic health risk indices related to water consumption.

4.3.1. Chronic daily intake

The majority of PTMs enter the body through a number of different routes, including ingestion, inhalation, and cutaneous exposure. The most prominent route for PTMs to reach the human body is by oral intake. According to the equation modified by Khan *et al.* (2013a) and Khan, Shahnaz *et al.* (2013b), the CDI of PTMs by drinking groundwater was computed as follows:

$$\mathrm{CDI} = \mathrm{CPTMs} \times \left(\frac{\mathrm{DIP\,TMs}}{\mathrm{bw}}\right) \tag{4}$$

In this formula, CPTMs stand for PTM concentrations, DIPTMs for daily water intake and bw for body weight. For adults and children, respectively, the projected daily groundwater consumption rates were 2 and 1 l/day, while the assumed average body weights were 70 and 20 kg, respectively.

4.3.2. Health risk index

The HRI of PTMs for humans is calculated by substituting the values of PTMs in the following equation as (USEPA 2005; Shah *et al.* 2012):

$$\mathrm{HRI} = \frac{\mathrm{CDI}}{\mathrm{RfD}} \tag{5}$$

RfD stands for the reference dose. Based on the estimated results, it was stated that the HRI values less than 1 revealed that there was no risk to humans posed by the ingestion of groundwater through drinking. The United States Environmental Protection Agency (USEPA 2005) defined the RfD as 'an estimate of a daily oral exposure to the human population that is likely to be without an appreciable risk of deleterious effects during a lifetime.' HRI levels greater than 1, however, indicate a risk to human health.

4.3.3. Carcinogenic analysis

Carcinogenic analysis of the probable cancer risks due to exposure to a specific dose of heavy metal in drinking water can be computed using the ILCR (Sultana *et al.* 2017). The ILCR is defined as the incremental probability of a person developing any type of cancer over a lifetime as a result of 24 h/day exposure to a given daily amount of a carcinogenic element for 70 years. The following equation (Equation (6)) was commonly used for the calculation of the lifetime cancer risk:

$$ILCR = CDI.CSF \tag{6}$$

where CSF is the cancer slope factor and is defined as the risk generated by a lifetime average amount of 1 mg/kg/day of carcinogen chemical and is contaminant specific. The permissible limits are considered to be 10^{-6} and $<10^{-4}$ for a single carcinogenic element and multi-element carcinogens (Tepanosyan *et al.* 2017).

5. RESULTS AND DISCUSSION

5.1. Descriptive statistics of hydrochemical parameters

Table 1 shows the descriptive statistics of the physicochemical characteristics and trace element results of drainage and groundwater collected in El Sharqia Governorate, with minimum, maximum, and average values for all parameters in the quaternary aquifer compared with guideline values set by the Environmental Protection Agency (USEPA 2009) and WHO WHO (2017) guidelines for drinking water purposes. These results indicate the following:

- The average pH of groundwater samples was 7.58, with values ranging from 7.06 to 8.19. The pH ranged from 6.54 to 7.6, with an average value of 7.08, for drainage water samples. The results showed circumstances that ranged from being slightly acidic to slightly alkaline, which may be related to pollution issues.

Table 1 | Descriptive statistics of physiochemical characteristics and trace element results of collected water samples

	Element	Min.	Max.	Average	SD		Min.	Max.	Average	SD	WHO (2017)
Groundwater	Na(meq/l)	1.30	10.00	4.86	50.36	Drainage water	3.04	12.61	6.43	49.99	8.696
	K (meq/l)	0.05	1.45	0.20	11.79		0.18	1.28	0.5	7.907	0.256
	Mg (meq/l)	1.01	6.86	3.40	22.16		0.81	7.57	3.73	20.14	2.500
	Ca (meq/l)	0.81	8.98	3.43	38.29		1.61	8.3	3.45	23.72	3.750
	CO_3 (meq/l)	0.00	2.24	0.85	20.24		0	0.98	0.23	8.29	
	HCO_3 (meq/l)	2.24	7.42	4.73	93.7		2.1	10.92	5.7	121.79	4.918
	SO_4 (meq/l)	0.12	5.20	2.29	83.02		1.04	6.66	3.19	65.29	10.417
	Cl (meq/l)	0.68	12.23	4.18	114.45		2.33	10.96	5.21	63.75	7.042
	$NH4^+$ (mg/l)	1.96	54.88	13.32	13.6		3.92	41.16	22.83	9.31	0.5
	NO_2 (mg/l)	0	2.17	0.2883	0.5		0.014	0.925	0.221	13.8	
	NO_3 (mg/l)	1.96	37.24	17.44	10.18		0	56.84	21.9	0.178	45
	PO_4 (mg/l)	0.01	0.61	0.295	0.156		0.023	0.502	0.2488	0.11	
	F (mg/l)	2.4	16	8.64	5.39		1.6	41.6	13.82	10.5	
	BOD (mg/l)	0.00083	0.031	0.0108	0.008		0.00083	0.0366	0.0158	0.0103	
	COD (mg/l)	0	140	33.04	39.27		0	240	67.56	50.66	
	TOC (mg/l)	0	0.0381	0.0098	0.008		0	0.0902	0.01137	0.0153	
	Turbidity (NTU)	0.36	11.95	4.011	3.42		1.09	52.2	18.81	13.18	
	TSS	0	30	11.91	10.9		2	668	71.02	114.7	
	Oil and grease	0	161	56.04	43.11		0	160	65.27	44.43	
	pH	7.06	8.19	7.58	0.279		6.54	7.6	7.08	0.277	
	EC (μS/cm)	363	2,268	1,124	520		872	2,083	1,373	283.75	
	TDS (mg/l)	214	1,227	650	293		421	1,401	796	199.34	1,000
	Ag (mg/l)	0.006	0.054	0.030			0.009	0.093	0.033		
	Al (mg/l)	0.023	0.776	0.231	0.18		0.028	5.703	0.654	0.96	
	B (mg/l)	0.008	0.192	0.072			0.030	0.189	0.084		
	Ba (mg/l)	0.019	0.286	0.139	0.08		0.003	0.165	0.074	0.04	
	Cd (mg/l)	0.003	0.026	0.010	0.006		0.001	0.040	0.012	0.008	
	Co (mg/l)	0.002	0.041	0.016	0.01		0.002	0.036	0.015	0.009	
	Cr (mg/l)	0.027	0.051	0.041	0.01		0.011	0.043	0.025	0.009	
	Cu (mg/l)	0.008	0.216	0.084	0.05		0.014	0.202	0.070	0.05	
	Fe (mg/l)	0.035	1.762	0.609	0.53		0.020	5.622	1.099	1.08	
	Mn (mg/l)	0.019	2.273	0.601			0.003	0.376	0.222		
	Mo (mg/l)	0.004	0.106	0.055			−0.044	0.117	0.055		
	Ni (mg/l)	0.002	0.056	0.033	0.01		0.005	0.059	0.030	0.014	
	Pb (mg/l)	0.041	0.160	0.117	0.06		0.009	0.266	0.094	0.066	
	Si (mg/l)	5.253	20.390	11.046			0.151	9.789	5.889		
	Sr (mg/l)	0.110	1.748	0.710	0.42		0.023	8.370	1.176	1.47	
	V (mg/l)	0.018	0.117	0.056			0.012	0.203	0.059		
	Zn (mg/l)	0.002	0.570	0.151	0.13		−0.005	0.524	0.094	0.09	

- The fact that drainage water had higher EC and TDS levels than groundwater may be attributable to anthropogenic pollution inputs. With an average of 1,373 μS/cm, the EC of drainage water ranged from 872 to 2,083 μS/cm. The average EC in groundwater samples was 1,124 μS/cm, with values ranging from 363 to 2,268 μS/cm. 19% of the collected samples had TDS values above the WHO (2017) standard limits for drinking water, which varied from 214 to 1,226 mg/l. TDS concentrations in drainage water samples ranged from 422 to 1,401 mg/l, exceeding WHO (2017) guidelines for drinking purposes by 12% (Table 1). In accordance with WHO salinity classifications from 2017, about 81% of groundwater samples and 89% of drainage water were categorized as fresh water, while 19 and 11%, respectively, were classified as somewhat saline.
- The relative abundance of major cations in shallow groundwater is $Na^+ > Mg^{2+} > Ca^{2+} > K^+$ (on a molar basis) and $HCO_3^- > Cl^- > SO_4^{2-}$ for anions by 43 and 38%, respectively. For drainage water samples, the predominant cations are $Na^+ > Mg^{2+} > Ca^{2+} > K^+$ (on a molar basis) and $HCO_3^- > Cl^- > SO_4^{2-}$ for anions by 51 and 57%, respectively.

- However, the maximum Ca^{2+} and Mg^{2+} concentrations in groundwater samples, 180 and 83 mg/l, respectively, are greater than WHO (2004) guideline limits by 38 and 62%, respectively. With the exception of sample number 54 (Na = 230 mg/l), the maximum sodium concentaration values are 230 mg/l within the established limits. However, groundwater samples have potassium concentrations of 57 mg/l, which are 14% higher than WHO (2004) limits. The maximum salt and potassium values in drainage water are 12 and 97%, respectively, above WHO guideline limits. HCO_3^- ions present in shallow groundwater samples may be due to the dissolution of carbonate rocks, soils, and atmospheric carbon dioxide.
- The first dominating anion in the study area is the bicarbonate ion. The lacustrine deposits present in the quaternary aquifer may be the source of the majority of Cl^- in the groundwater. Sedimentary rocks like gypsum ($CaSO_4.2H_2O$) and anhydrite ($CaSO_4$), which permit active dissolving, leaching, and ion-exchange processes, are the most prevalent and significant occurrences of sulfate ions in the researched area. The breakdown of organic matter in the soil and the addition of leachable sulphate in fertilizers used in intensively farmed areas are two additional sources of sulphate addition to groundwater.

5.2. Assessment of pollution indicators in collected water samples

The environmental impacts of anthropogenic pollution on the general water resources quality in the study area will be evaluated according to the variations of ammonia, nitrate, phosphate, BOD, OD, TOC oil, and grease with spatial distribution as shown in Figures 4 and 5 and Table 1 as follows:

- The breakdown of organic substances containing nitrogen can produce ammonia in water. The main causes of ammonia contamination in the environment are the discharge of agricultural, industrial, and sewage effluent. Ammonia levels in the water are a sign of potential bacterial, sewage, and animal waste pollution. The tested groundwater and drainage water samples have ammonia concentrations that range from 1.96 to 54.88 mg/l and from 3.94 to 41.16 mg/l, respectively. All of these samples are above the NH_4^+ drinking water maximum suggested level of 0.5 mg/l. While nitrate is a naturally occurring substance in the environment, nitrite is rarely seen in large concentrations. However, nitrate can reduce to nitrite, and in reducing environment, toxicological effects could manifest. Agricultural practices, wastewater transporting human and animal excrement, and other factors can create nitrate contamination even though nitrate may be present in the environment naturally (Boyacioglu 2007; WHO 2011). Nitrate levels in the drainage water samples and groundwater samples that were examined ranged from 0 to 56.84 mg/l and 1.96 to 37.24 mg/l, respectively. Most drainage water samples are above the acceptable maximum limit (WHO 2017).
- Anthropogenic sources are responsible for high NO_3^-, PO_4^{3-}, and Cl^- concentrations as illustrated in Figure 3 for the relationships of NO_3 vs. PO_4 and NO_3 vs. Cl in (mg/l), respectively, in both drainage and groundwater samples.
- Dissolution/precipitation of organic materials and the presence of some metallic compounds like iron, manganese, and chromium, and the discharge of industrial effluents into surface water are just a few of the variables that can affect the turbidity and color of water systems. Color changes that result from these factors could potentially signal a dangerous issue (WHO 2011). Organic and/or inorganic substances that are suspended or colloidal in the water can also produce turbidity. Turbidity can be a symptom of potential microbial contamination because bacteria can cling to particles (TSE 1998; Cude

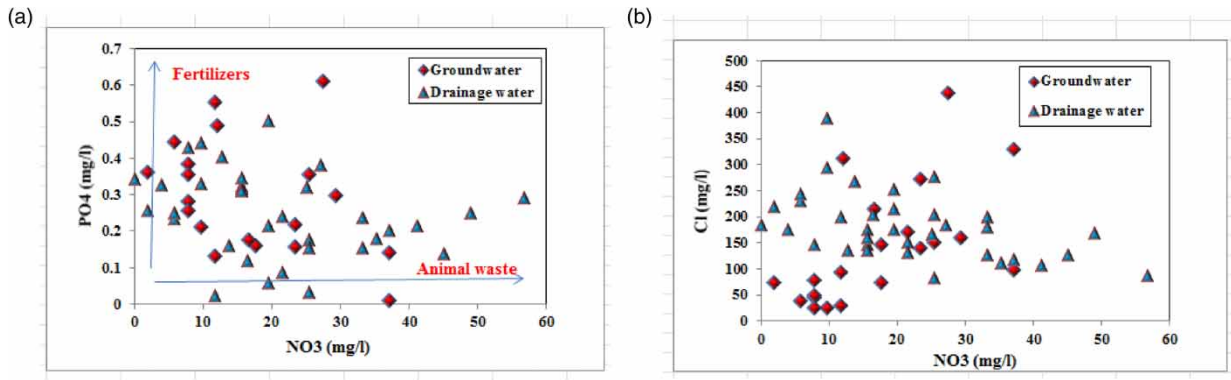

Figure 3 | Relationships of (a) NO_3 vs. PO_4 and (b) NO_3 vs. Cl in (mg/l).

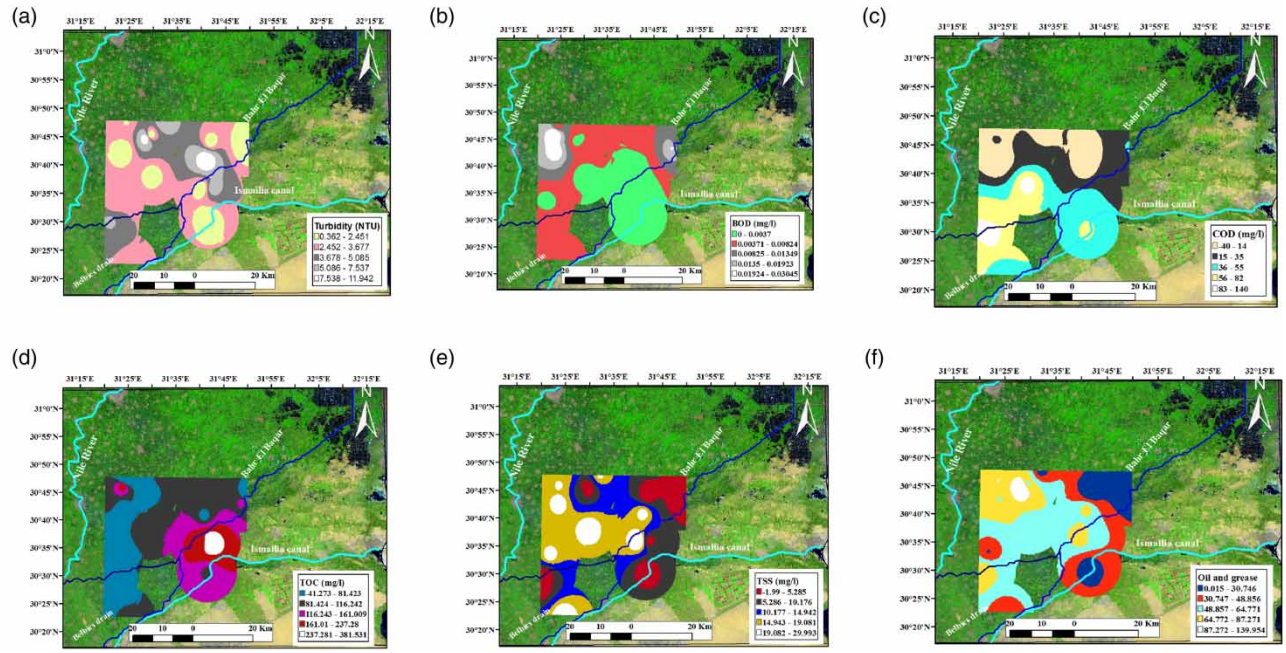

Figure 4 | Spatial distribution of (a) turbidity; (b) BOD; (c) COD; (d) TOC; (e) TSS; and (f) oil and grease for groundwater.

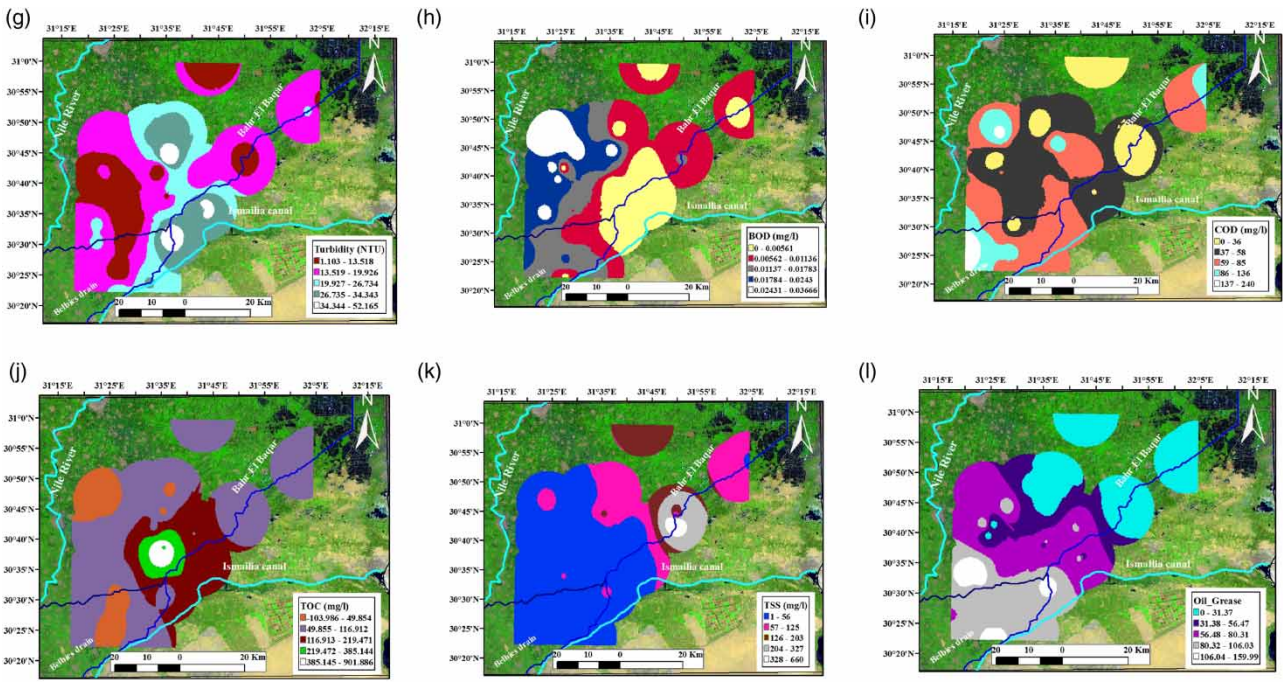

Figure 5 | Spatial distribution of (g) turbidity; (h) BOD; (i) COD; (j) TOC; (k) TSS; and (l) oil and grease for drainage water.

2001; WHO 2011; Akkoyunlu & Akiner 2012). The groundwater's mean value is below the allowable limit, according to the results for color and turbidity. As seen in Table 1 and Figures 4 and 5 drainage water has issues with turbidity, color, and/or clarity.

- The water body has been contaminated by both oxidizable organic and inorganic contaminants, according to the COD and TOC readings (Mohamed *et al.* 2015). The mean COD of groundwater and drainage water is 33.04 and 67.6 respectively.

Figures 4 and 5 reflect the degraded groundwater quality in this zone as a result of continuous sewage disposal in the study area especially around the main drains (Bahr El Baqr and Belbies). Poor water quality is indicated by high BOD values, which are associated with waste discharges that contain increased microbial activity brought on by the degradation of organic materials, as well as organic and nutritional content. In all of the wells assessed during the monitoring, BOD values were less than 5.0 mg O_2 L^{-1}.

- For drainage and groundwater samples, it was found that some trace elements, including Al, Fe, Mn, Pb, Si, and Sr, exceeded WHO limits for drinking purposes.
- The concentrations of iron in the analyzed groundwater and drainage water samples vary from 0.03 to 1.76 mg/l and from 0.02 to 5.62 mg/l, respectively. All these samples exceed the maximum recommended limit for Fe^{3+} in drinking water (0.3 mg/l) where various iron salts are used as coagulating agents in water-treatment plants and cast iron, steel, galvanized iron pipes are used for water distribution.
- The concentrations of Mn^{2+} in drainage and groundwater vary from 0.002 to 0.376 and 0.018 to 2.27 mg/l, respectively. Most of these samples exceed the maximum recommended limit for Mn^{2+} in drinking water which may be due to the discharge of industrial effluents from the steel and iron factories. Lead was one of the first non-ferrous metals used by man. It has been used in many industrial applications such as batteries and cable sheeting. Lead does not appear to be an essential element for life for any organism. It is less toxic to plants than mercury and copper, with adverse effects being noted at concentration levels between 100 and 5,000 μg/l.
- Lead is toxic to humans. It substitutes calcium in bone and accumulates in it. Lead poisoning is manifested by anemia, kidney disease, and disturbances of the central nervous system. Lead poisoning suffered in childhood may cause mental retardation and convulsions in later life. The limit of lead in drinking water is 0.01 mg/l (WHO 2011). Lead concentrations varied between 0.04–0.159 mg/l and 0.009–0.266 mg/l in groundwater and drainage water, respectively. The results suggested that most of the mean values of trace elements in drainage water were higher than those in groundwater. It could manifest that surface water exhibited relatively more pollution problems.

5.3. Geochemical modeling

Using the PHREEQC software, a geochemical model was created for potential hydrochemical reactions along the flow routes (Parkhurst & Appelo 1999). Groundwater solutes may be produced by three geochemical processes: evaporation, carbonate dissolution/precipitation, and silicate weathering (Garrels & MacKenzie 1971). Table 2 shows statistical outcomes of the saturation index of drainage and groundwater samples using PHREEQC. The findings showed that several minerals and gases, such

Table 2 | Statistical results of the saturation index for the collected drainage and groundwater samples

Minerals			Min.	Max.	Average		Min.	Max.	Average
Calcite	$CaCO_3$	Groundwater	−0.493	0.848	0.29	Drainage water	−5.818	0.277	−0.45
Dolomite	$CaMg(CO_3)_2$		0.04	2.773	1.67		−10.302	1.758	0.22
Cerussite	$PbCO_3$		− 0.905	− 0.37	− 0.56		− 1.714	− 0.297	− 0.85
Smithsonite	$ZnCO_3$		−3.122	−0.182	−1.40		−8.729	−1.146	−2.46
Strontianite	$SrCO_3$		−2.225	−0.581	−1.32		−7.546	−0.1	−2.13
Witherite	$BaCO_3$		−3.81	−1.872	−2.87		−9.18	−0.045	−3.64
Siderite	$FeCO_3$		− 0.757	0.749	− 0.18		− 6.369	0.79	− 0.68
Rhodochrosite	$MnCO_3$		− 1.769	0.794	− 0.22		− 7.461	0.004	− 1.23
Anhydrite	$CaSO_4$		−3.697	−1.385	−2.23		−7.171	−1.278	−2.19
Gypsum	$CaSO_4$		−3.407	−1.096	−1.94		−5.323	0.221	−1.71
Barite	$BaSO_4$		−1.333	0.757	0.10		−7.859	0.767	−0.45
Celesite	$SrSO_4$		−4.08	−1.621	−2.51		−11.747	−1.357	−2.93
Halite	NaCl		−7.603	−5.834	−6.63		−6.834	3.917	−5.46
Gibbsite	$Al(OH)_3$		1.837	4.272	3.17		2.323	4.642	3.67

as cerussite, smithsonite, strontianite, witherite, anhydrite, gypsum, celesite, and halite, were undersaturated in the drainage and groundwater samples of the quaternary aquifer, requiring dissolution to bring them into equilibrium. Minerals/gases like calcite, dolomite, siderite, rhodochrosite, barite, and gibbsite have a propensity to precipitate in drainage and groundwater samples.

5.4. Multivariate statistical analyses

With support for a wide range of factors, SPSS version 22.0 software was used to perform mathematical and statistical computations on the data (Matiatos *et al.* 2014).

5.4.1. Factor analysis

A statistical method for examining the correlations between numerous variables is factor analysis. This strategy entails minimizing information loss while condensing the data from a large number of original variables into a more manageable set of uncorrelated main components (factors) (Hair *et al.* 1992; Abu Salem *et al.* 2017; El Alfy *et al.* 2018).

5.4.2. Principal component analysis

Principal component analysis (PCA) was done to determine the mechanisms controlling ion concentrations. The factor loadings of each original variable were investigated after extracting factors with eigenvalues greater than 1 (Kaiser 1960). Eight distinct components that account for the majority of the variability were identified using eigenvalues and varimax rotation. According to Table 3, the overall variance for the water samples was around 73.17%. Statistically, the first dominant factor (F1) is responsible for 20.79% of the variance in the data. Strongly positive loadings on EC, TDS, hardness, Na, SO_4, Cl, and

Table 3 | Loadings of the experimental variables on the significant principal component analysis (PCA)

	PC1	PC2	PC3	PC4	PC5	PC6	PC7	PC8
pH	− 0.600	− 0.163	− 0.129	− 0.035	0.515	0.063	− 0.091	0.052
EC	0.948	− 0.076	− 0.063	− 0.054	0.135	− 0.090	0.053	0.015
TDS	0.967	− 0.122	− 0.034	− 0.038	0.126	− 0.081	− 0.002	0.003
Hardness	− 0.259	− 0.126	0.209	0.703	0.206	− 0.243	0.136	− 0.017
Na	0.864	− 0.192	0.089	− 0.080	0.132	0.076	0.016	− 0.013
SO_4	0.862	− 0.018	− 0.080	0.159	0.117	0.155	− 0.051	0.046
Cl	0.877	− 0.041	− 0.030	− 0.037	0.075	− 0.260	0.150	− 0.065
Al	0.036	0.660	− 0.293	0.262	− 0.051	0.270	− 0.239	− 0.181
Cd	− 0.104	0.234	0.715	− 0.251	− 0.166	0.142	0.119	− 0.193
Co	0.007	0.354	− 0.081	− 0.539	0.225	0.330	0.224	0.089
Cr	0.044	0.524	− 0.306	0.191	0.351	− 0.063	0.065	− 0.371
Fe	0.180	0.592	0.557	0.239	− 0.077	0.097	− 0.161	− 0.002
Ni	0.170	− 0.023	− 0.125	0.039	− 0.468	− 0.306	− 0.363	− 0.294
Pb	− 0.164	− 0.098	− 0.029	0.145	− 0.234	− 0.030	0.733	− 0.397
Sr	− 0.047	0.363	− 0.081	0.080	0.149	− 0.435	0.128	0.498
NO_2	0.071	− 0.253	0.011	0.643	0.055	0.299	0.233	0.317
NO_3	− 0.023	0.670	− 0.050	− 0.032	0.432	− 0.071	0.200	0.015
NH_4	0.238	0.398	0.022	− 0.071	− 0.477	− 0.015	0.385	0.098
TSS	0.163	0.329	0.828	0.017	0.139	0.045	− 0.105	0.130
COD	0.184	0.570	− 0.409	0.251	− 0.116	0.353	− 0.075	− 0.037
TOC	0.158	− 0.211	− .029	0.261	− 0.388	0.490	− 0.005	0.228
S	− 0.016	0.409	− 0.012	0.212	− 0.310	− 0.506	− 0.071	0.138
Oil–grease	− 0.110	0.272	− 0.338	− 0.320	− 0.323	− 0.042	0.075	0.394
% of Variance	20.795	12.500	9.061	7.725	7.330	6.055	5.048	4.659
Cumulative %	20.795	33.296	42.356	50.081	57.411	63.465	68.513	73.172

pH are characteristics of this component. pH has a substantially negative loading. This element, which might also be called the salinity factor, reveals the impact of lithogenesis on the groundwater. The influence of sewage contamination can be seen in the second factor (F2), which accounts for 10.02% of the overall variation. It exhibits high positive loadings on Al and COD as well as moderately positive loadings on nitrate and Cr. Additionally, the third factor (F3) exhibits substantial positive loadings on Fe and TSS, indicating anthropogenic input for these elements, and it describes 9.72% of the overall variance. A strong positive loading on Na, a moderately negative loading on Co, oil, and grasses, and a moderately positive loading on NO_2 are all displayed by the fourth factor (F4), which accounts for 7.98% of the overall variation. With a substantial positive loading on Ni and Zn, the fifth factor (F5), which explains 8% of the overall variance, demonstrates anthropogenic impacts on groundwater. The final factor (F6), which contributes 7% of the overall variation, exhibits a high negative loading on Cd and a moderately positive loading on Cr (Table 3).

One method for identifying various classes and groupings within the studied data is hierarchical cluster analysis (HCA), with the outcomes shown as a dendrogram (Davis 1986). According to the proximity of the water quality measures, the

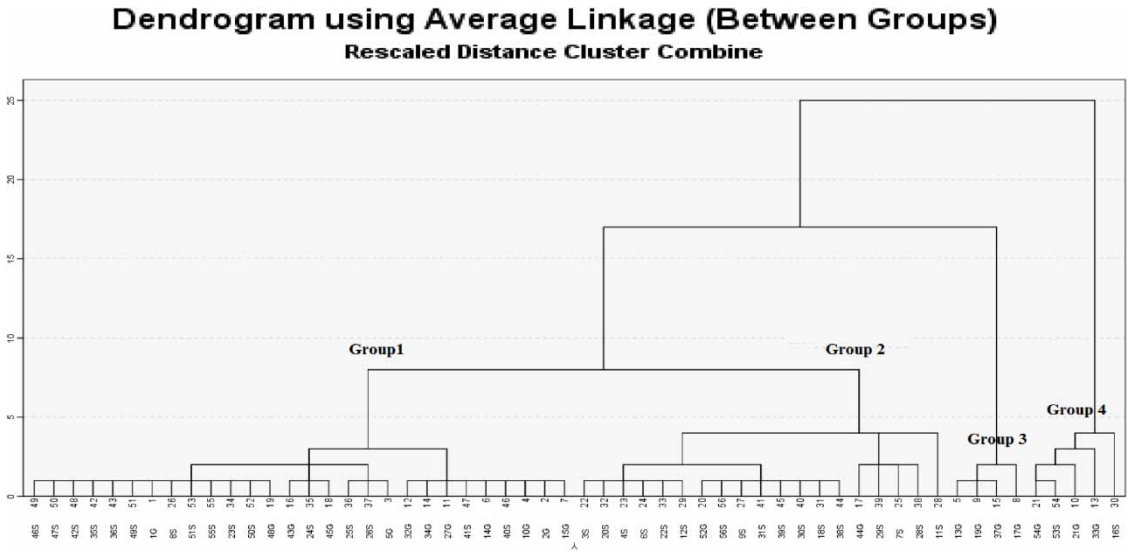

Figure 6 | Q-mode cluster analysis dendrogram for 56 samples and 23 chemical variables.

Table 4 | Parameter values of the four principal water groups

	Group 1			Group 2			Group 3			Group 4		
	Min.	Max.	Average	Min.	Max.	Average	Min.	Max.	Average	Min.	Max.	Average
pH	6.54	8	7.35	6.63	7.6	7.05	7.23	8.19	7.705	7	7.6	7.269
EC (μS/cm)	788	1,275	1,055	1,339	1,815	1,532	363	648	506	1,999	2,268	2,099
TDS (mg/l)	422	810	605	773	1,051	898	214	338	284	1,088	1,401	1,224
Ca (mg/l)	36.36	101	61.37	32.3	166	77.03	16.16	36.36	26	78.9	180	111
Mg (mg/l)	9.8	72	37.65	12.63	78.53	48.23	12	27	18.5	58	92	77
Na (mg/l)	30	150	102	120	220	170.8	32	86	59.33	150	290	213
K (mg/l)	2	30	13.3	5	31	17.47	2	8	4.667	6	57	29
CO_3 (mg/l)	0	67.2	16.8	0	29.4	5.8	0	42	18.2	8.4	50.4	28.8
HCO_3 (mg/l)	128	504	306	153	614	348	137	324	226	205	666	427
SO_4 (mg/l)	30	210	100.6	80	320	189	6	30	17.3	170	300	236
Cl (mg/l)	24.29	185	120	145.7	330	222	24.29	44	34	214	437	322

analyzed groundwater samples have been divided into four primary clusters: 1, 2, 3, and 4 as shown in (Figure 6). Total dissolved solids (TDS) and ionic composition, which are governed by hydrogeochemical and physicochemical circumstances, form the basis for the clustering of these samples.

5.5. Modeling of mixing groups

The clustering procedure was carried out by the Ward's linkage approach using the Euclidean distance as a measure of sample similarity, which was based on the clustering Q-technique, in which similarity associations among water samples were explored. Figure 6 shows the dendrogram's findings. Based on the dendrogram classification, four preliminary groupings were chosen. With an average value for each metric shown in Table 4, each group represents a hydrochemical facies.

Two triangles, one for cations and the other for anions, as well as a diamond-shaped region for both cations and anions are included in the Piper trilinear diagram (Piper 1994). Major cations (Ca^{+2}, Mg^{+2}, and $Na^{+} + K^{+}$) and major anions (Cl^{-}, SO_4 and HCO_3^{-}), as determined by chemical analysis, are plotted in the diamond shape (stated as meq/l). Figure 7 shows the outcomes of the four groups' chemical analyses. Except for a few examples of group 2 (Na–Cl) and group 3 ($Mg–HCO_3$) water types, the majority of the groups are made up of mixed water types.

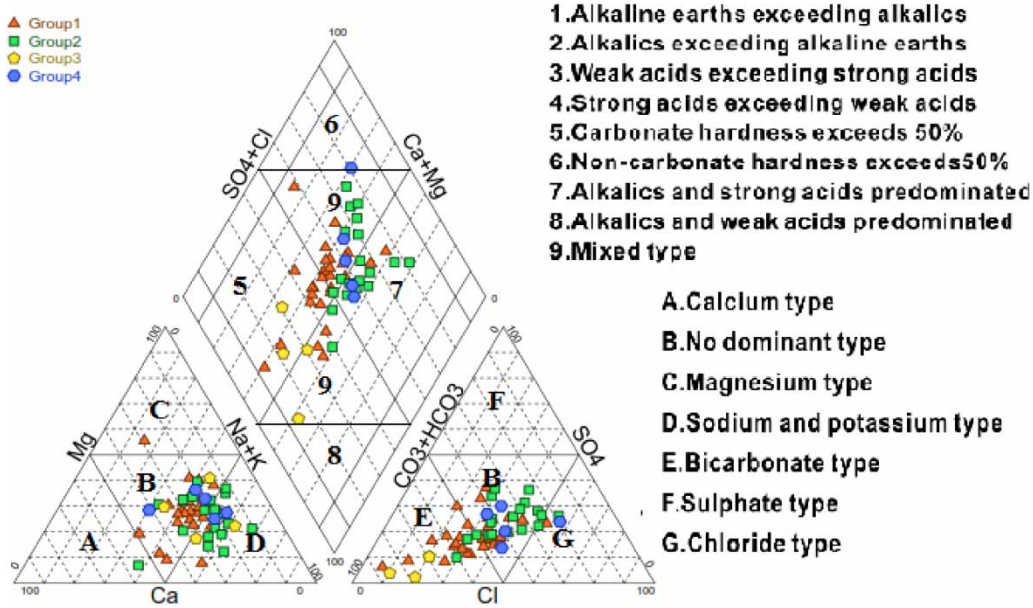

Figure 7 | Piper diagram for water samples.

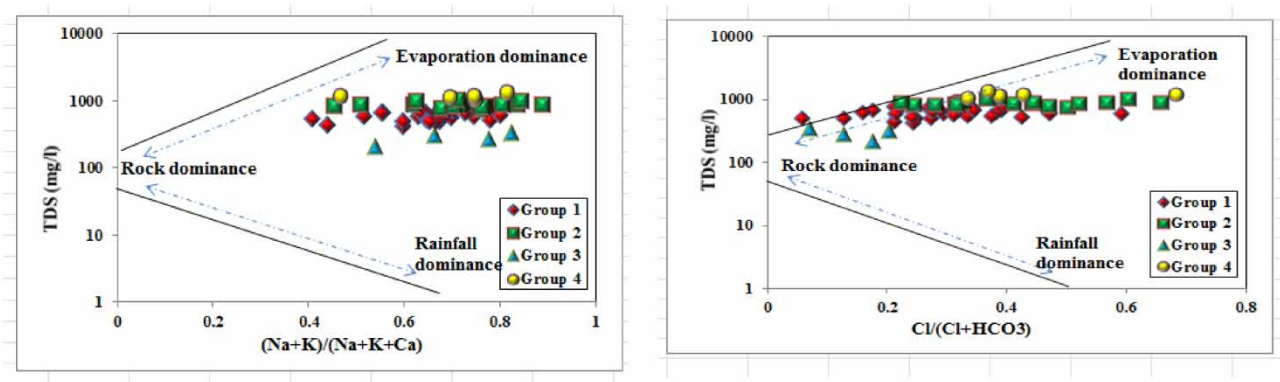

Figure 8 | Gibbs plot for the four principal water groups.

Table 5 | Modeled major ion concentrations between the four principal water groups (expressed in molality)

Mixing groups	HCO_3	Ca	Cl	K	Mg	Na	SO_4
90% Group 1: 10% Group 2	0.004036	0.000897	0.001028	0.000059	0.000415	0.001697	0.000365
10% Group 1: 90% Group 2	0.003726	0.000816	0.003769	0.000120	0.000508	0.004831	0.000781
80% Group 1: 20% Group 2	0.003997	0.000887	0.001371	0.000067	0.000427	0.002089	0.000417
20% Group 1: 80% Group 2	0.003765	0.000827	0.003427	0.000113	0.000497	0.004439	0.000729
70% Group 1: 30% Group 2	0.003958	0.000877	0.001713	0.000074	0.000438	0.002480	0.000469
30% Group 1: 70% Group 2	0.003803	0.000837	0.003084	0.000105	0.000485	0.004047	0.000677
50% Group 1: 50% Group 2	0.003881	0.000857	0.002399	0.000090	0.000462	0.003264	0.000573
90% Group 2: 10% Group 3	0.003625	0.000766	0.003769	0.000120	0.000517	0.004840	0.000756
10% Group 2: 90% Group 3	0.003130	0.000444	0.001028	0.000059	0.000496	0.001775	0.000140
80% Group 2: 20% Group 3	0.003563	0.000726	0.003427	0.000113	0.000515	0.004457	0.000679
20% Group 2: 80% Group 3	0.003192	0.000484	0.001371	0.000067	0.000499	0.002158	0.000217
70% Group 2: 30% Group 3	0.003501	0.000685	0.003084	0.000105	0.000512	0.004073	0.000602
30% Group 2: 70% Group 3	0.003254	0.000524	0.001713	0.000074	0.000502	0.002541	0.000294
50% Group 2: 50% Group 3	0.003377	0.000605	0.002399	0.000090	0.000507	0.003307	0.000448
90% Group 3: 10% Group 4	0.003160	0.000560	0.001221	0.000061	0.000683	0.001906	0.000233
10% Group 3: 90% Group 4	0.003903	0.001814	0.005506	0.000143	0.002198	0.006017	0.001600
80% Group 3: 20% Group 4	0.003253	0.000717	0.001757	0.000072	0.000873	0.002420	0.000404
20% Group 3: 80% Group 4	0.003810	0.001657	0.004970	0.000133	0.002009	0.005503	0.001429
70% Group 3: 30% Group 4	0.003346	0.000873	0.002292	0.000082	0.001062	0.002934	0.000575
30% Group 3: 70% Group 4	0.003717	0.001500	0.004435	0.000123	0.001820	0.004989	0.001259
50% Group 3: 50% Group 4	0.003532	0.001187	0.003363	0.000102	0.001441	0.003961	0.000917
90% Group 1: 10% Group 4	0.004066	0.001014	0.001221	0.000061	0.000602	0.001828	0.000458
10% Group 1: 90% Group 4	0.004003	0.001864	0.005506	0.000143	0.002189	0.006008	0.001625
80% Group 1: 20% Group 4	0.004059	0.001120	0.001757	0.000072	0.000800	0.002350	0.000604
20% Group 1: 80% Group 4	0.004011	0.001758	0.004970	0.000133	0.001991	0.005485	0.001479
70% Group 1: 30% Group 4	0.004051	0.001226	0.002292	0.000082	0.000999	0.002873	0.000750
30% Group 1: 70% Group 4	0.004019	0.001651	0.004435	0.000123	0.001792	0.004963	0.001334
50% Group 1: 50% Group 4	0.004035	0.001439	0.003363	0.000102	0.001395	0.003918	0.001042
90% Group 2: 10% Group 4	0.004463	0.000923	0.004305	0.000131	0.000707	0.005353	0.000927
10% Group 2: 90% Group 4	0.004047	0.001854	0.005849	0.000151	0.002201	0.006400	0.001677
80% Group 2: 20% Group 4	0.004411	0.001039	0.004498	0.000133	0.000893	0.005484	0.001021
20% Group 2: 80% Group 4	0.004099	0.001738	0.005656	0.000149	0.002014	0.006269	0.001584
70% Group 2: 30% Group 4	0.004359	0.001156	0.004691	0.000136	0.001080	0.005615	0.001115
30% Group 2: 70% Group 4	0.004151	0.001621	0.005463	0.000146	0.001827	0.006138	0.001490
50% Group 2: 50% Group 4	0.004255	0.001388	0.005077	0.000141	0.001454	0.005876	0.001302
90% Group 1: 10% Group 3	0.003918	0.000857	0.000685	0.000051	0.000412	0.001314	0.000287
10% Group 1: 90% Group 3	0.002666	0.000454	0.000685	0.000051	0.000485	0.001384	0.000087
80% Group 1: 20% Group 3	0.003761	0.000807	0.000685	0.000051	0.000421	0.001323	0.000262
20% Group 1: 80% Group 3	0.002823	0.000504	0.000685	0.000051	0.000476	0.001375	0.000113
70% Group 1: 30% Group 3	0.003605	0.000756	0.000685	0.000051	0.000430	0.001331	0.000237
30% Group 1: 70% Group 3	0.002979	0.000555	0.000685	0.000051	0.000467	0.001366	0.000137
50% Group 1: 50% Group 3	0.003292	0.000655	0.000685	0.000051	0.000448	0.001349	0.000187

In order to distinguish between samples whose chemical composition is primarily changed by freshwater dilution, rock weathering or evaporation/precipitation, Gibbs (1970) devised a presentation. This is based on the relationship between TDS and the cationic and anionic sides' respective ratios of $(Na/(Na + K)$ or $(Cl/(Cl + HCO_3)$. The distribution of the four main water groups under study on Gibbs diagrams (Figure 8) illustrates how evaporation and rock/water interaction mechanisms dominate the salt composition.

The first group of water, group 1, has salinity ranging from 422 to 810 mg/l with an average value of 605 mg/l with abundance orders (meq/l) of $Na^+ > Mg^{2+} > Ca^{2+} > K^+$ and $HCO_3^- > Cl^- > SO_4^{2-} > CO_3^{2-}$. This water group is classified as HCO_3^- alkaline earth water type. This is probably derived from carbonate precipitation. For group 2, the salinity of water samples varied from 773 to 1,051 mg/l with an average value of 898 mg/l, while for group 3, the salinity ranged from 214 to 338 mg/l with an average value of 284 mg/l (freshwater). For group 4 water samples, the cationic composition was dominated by Na^+ and Mg^{2+} followed by Ca^{2+} and K^+ and $Cl^- > HCO_3^- > SO_4^{2-} > CO_3^{2-}$ and high salinity ranged from 1,088 to 1,401 mg/l with an average value of 1,224 mg/l. Applying mixing process simulation between the four principal water groups using PHREEQC software is to indicate precisely the routes of mixing sources within the quaternary aquifer in El Sharqia Governorate. The geochemical modeling results shown in Table 5 illustrate that simulation of a double-mixing process (20% Group 1:80% Group 4) leads to calcium contents similar to those of samples 24 and 36. Also, mixing of 10% Group

Table 6 | Non- carcinogenic risks to humans from drainage and groundwater samples.

	Groundwater					
	Children			**Adult**		
Sample	**Min**	**Max**	**Average**	**Min**	**Max**	**Average**
Al	9.753×10^{-1}	7.571×10^{1}	1.497×10^{1}	7.663×10^{-1}	2.475×10^{1}	7.921
Cd	5.462×10^{-5}	2.060×10^{-3}	4.156×10^{-4}	4.400×10^{-5}	1.659×10^{-3}	3.348×10^{-4}
Co	1.951×10^{-3}	8.017×10^{-2}	2.002×10^{-2}	1.571×10^{-3}	6.459×10^{-2}	1.613×10^{-2}
Cr	1.300×10^{-1}	6.619×10^{-1}	2.438×10^{-1}	1.048×10^{-1}	5.332×10^{-1}	1.964×10^{-1}
Fe	1.115×10^{-3}	9.820×10^{-2}	2.818×10^{-2}	8.980×10^{-4}	7.911×10^{-2}	2.270×10^{-2}
Ni	3.901×10^{-4}	1.092×10^{-2}	2.489×10^{-3}	3.143×10^{-4}	8.800×10^{-3}	2.005×10^{-3}
Pb	0.000	1.730	7.750×10^{-1}	6.984×10^{-2}	1.393	6.762×10^{-1}
Sr	7.179×10^{-3}	1.137×10^{-1}	4.617×10^{-2}	5.783×10^{-3}	9.156×10^{-2}	3.720×10^{-2}
Zn	1.040×10^{-4}	7.406×10^{-2}	1.619×10^{-2}	8.381×10^{-5}	5.966×10^{-2}	1.304×10^{-2}
Cu	8.541×10^{-3}	2.278×10^{-1}	8.844×10^{-2}	6.880×10^{-3}	1.835×10^{-1}	7.124×10^{-2}
Ba	3.609×10^{-3}	5.577×10^{-2}	2.713×10^{-2}	2.907×10^{-3}	4.493×10^{-2}	2.186×10^{-2}
	Drainage water					
Sample	**Min**	**Max**	**Average**	**Min**	**Max**	**Average**
Al	0.000	5.562×10^{2}	4.771×10^{1}	7.857×10^{-1}	9.366×10^{1}	1.856×10^{1}
Cd	5.462×10^{-5}	3.121×10^{-3}	5.319×10^{-4}	4.400×10^{-5}	2.514×10^{-3}	4.364×10^{-4}
Co	1.951×10^{-3}	6.944×10^{-2}	2.455×10^{-2}	1.571×10^{-3}	5.594×10^{-2}	1.977×10^{-2}
Cr	1.300×10^{-1}	5.553×10^{-1}	1.939×10^{-1}	1.048×10^{-1}	4.473×10^{-1}	1.562×10^{-1}
Fe	1.115×10^{-3}	3.133×10^{-1}	5.312×10^{-2}	8.980×10^{-4}	2.524×10^{-1}	4.279×10^{-2}
Ni	3.901×10^{-4}	1.145×10^{-2}	1.988×10^{-3}	3.143×10^{-4}	9.224×10^{-3}	1.602×10^{-3}
Pb	8.670×10^{-2}	2.886	5.922×10^{-1}	6.984×10^{-2}	2.325	4.771×10^{-1}
Sr	1.476×10^{-3}	5.442×10^{-1}	7.649×10^{-2}	1.189×10^{-3}	4.384×10^{-1}	6.162×10^{-2}
Zn	-7.022×10^{-4}	6.812×10^{-2}	1.022×10^{-2}	-5.657×10^{-4}	5.487×10^{-2}	8.232×10^{-3}
Cu	6.327×10^{-3}	2.127×10^{-1}	6.644×10^{-2}	5.097×10^{-3}	1.713×10^{-1}	5.352×10^{-2}
Ba	6.242×10^{-4}	3.226×10^{-2}	1.434×10^{-2}	5.029×10^{-4}	2.599×10^{-2}	1.155×10^{-2}

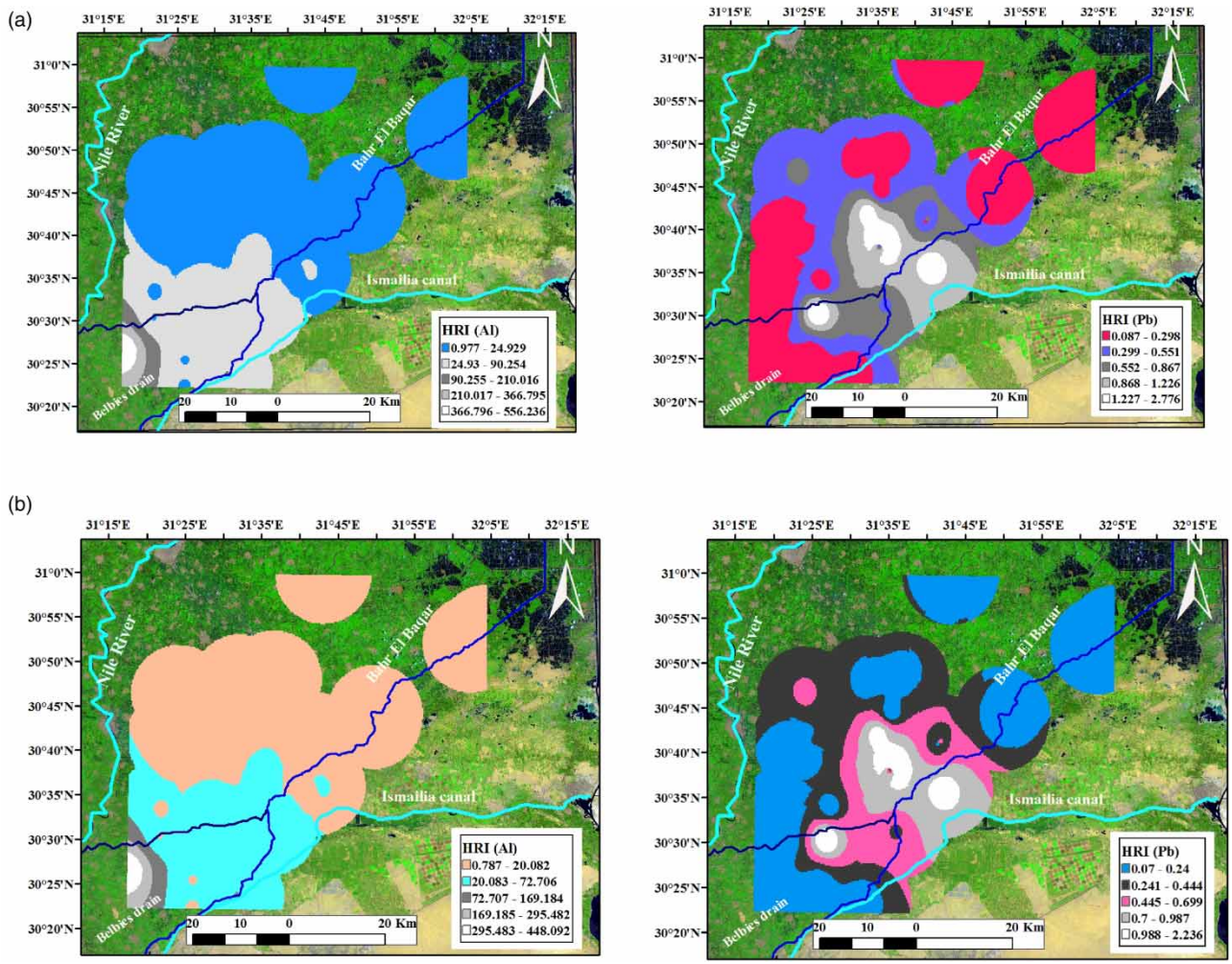

Figure 9 | (a) Spatial distribution of children HRI for Al and Pb of drainage water samples and (b) spatial distribution of adult Health Risk Index (HRI) for Al and Pb of drainage water samples.

1:90% Group 2 leads to chloride contents similar to those of samples 25, 35, 42, 46 and 49. Mixing of 90% Group 1:10% Group 2 gives sulphate contents similar to those of samples 28 and 53.

6. POTENTIAL HUMAN HEALTH RISK ASSESSMENT

6.1. Non-carcinogenic analysis

Results of trace elements analysis are illustrated in Table 1, where trace elements in groundwater samples were ranked as follows: Fe > Sr > Al > Zn > Ba > Cu > Pb > Ni > Cr > Co > Cd and for drainage water samples were ranked as follows: Sr > Al > Fe > Zn > Pb > Cu > Ba > Ni > Cr > Cd > Co according to their concentrations in mg/l. Examining HRI values for different age groups of people including children and adults in the study area are shown in Table 6 with spatial distribution of HRI values for both drainage and groundwater samples in Figures 9 and 10.

Results of the HRI of collected water samples reveal that all samples have HRI < 1 for all trace elements except Al and Pb which have HRI > 1 for both children and adults in drainage and groundwater samples. Spatial distribution of HRI values in Figures 9 and 10 of drainage and groundwater samples revealed that drainage water has higher HRI values than groundwater samples, especially near the drains with higher values for children than adults confirming that children are more sensitive to the adverse health effects of metals that have non-carcinogenic risks (USEPA 2012), because children are most likely to have oral intake by hand and mouth (Kusin *et al.* 2018).

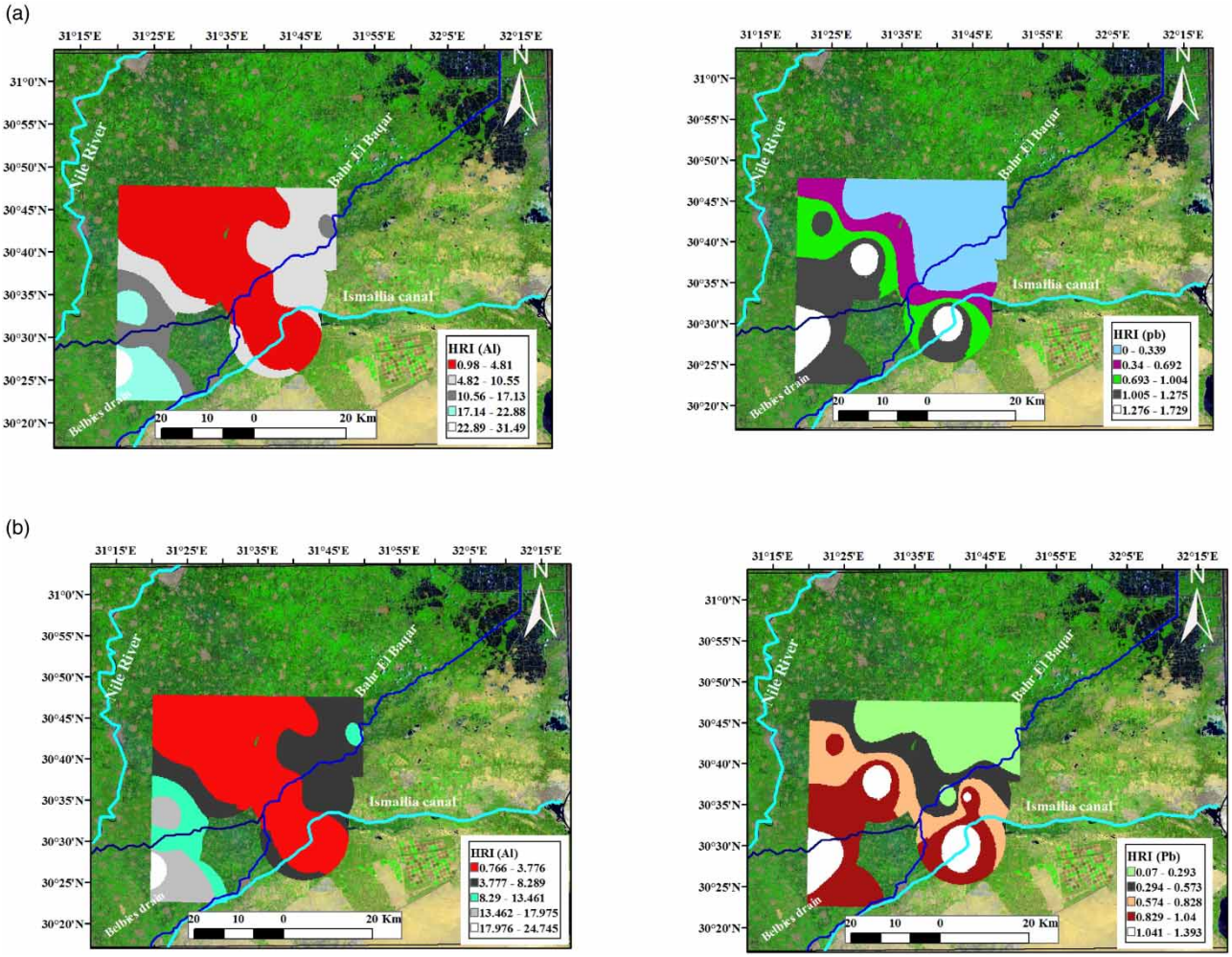

Figure 10 | (a) Spatial distribution of children HRI for Al and Pb of groundwater samples and (b) spatial distribution of adult Health Risk Index (HRI) for Al and Pb of groundwater samples.

6.2. Carcinogenic risk analysis

Heavy metals such as Cr, Ni and Pb can potentially enhance the risk of cancer in humans (Tani & Barrington 2005). Long-term exposure to low amounts of toxic elements could result in many types of cancer diseases. Using Cr, Ni, and Pb as carcinogens, the total exposure of the residents was calculated for groundwater samples used for drinking purposes as shown in Table 7.

For one heavy metal, an ILCR less than 1×10^{-6} is considered insignificant and the cancer risk can be neglected; while an ILCR above 1×10^{-4} is considered harmful and the cancer risk is troublesome. Results of Table 7 indicate that chromium

Table 7 | The incremental lifetime cancer risk (ILCR) values of carcinogenic human health risks via total exposure (ingestion and dermal contact) to the drinking water of the study area for adults

	ILCR		
	Cr	**Ni**	**Pb**
Min	1.675×10^{-6}	6.865×10^{-10}	1.389×10^{-7}
Max	8.527×10^{-6}	1.922×10^{-8}	2.772×10^{-6}
Average	3.141×10^{-6}	4.380×10^{-9}	1.345×10^{-6}

and lead may have a chance of cancer risk, while nickel has the lowest chance for cancer risk from the contaminants to resident's people.

7. CONCLUSION

This study was accomplished to appraise the main factors controlling water resources evolution/pollution indicators emphasizing direct/indirect human health risks in El Sharqia Governorate, Egypt. Most of the collected groundwater samples were shallow with depths ranging from 8 to 13 m, which implies that these wells are more vulnerable to contamination. Salinity classifications show that about 81% of groundwater samples and 89% of drainage water were freshwater, while about 19 and 11% were classified as slightly saline, respectively. Groundwater quality in the study area was controlled by natural processes (involving dissolution/precipitation of minerals, cation exchange, and evaporation) or anthropogenic factors (including leaching of solid waste, overuse of agricultural fertilizers, high loads of discharged sewage water) responsible for water quality deterioration. It was found that ammonia, nitrate, BOD, phosphate, turbidity, iron, manganese, lead, and aluminum values exceeded the limit of drinking water international standards. A human health risk was identified in the case of Pb and Al with high HRI values for different age groups of people including children and adults exceeding unity. It seems that the aquifer in the study area is quite vulnerable to pollution.

8. RECOMMENDATIONS

An advanced sanitary drainage network must be designed; chemical and bacteriological analyses must be carried out periodically for surface and groundwater to ensure the suitability of water for different purposes, taking into consideration the different hydrological and soil parameters that affect the susceptibility of the aquifer to pollution.

ACKNOWLEDGEMENTS

It is a pleasure to acknowledge the technical support provided by the Egyptian Atomic Energy Authority (EAEA), the Egyptian Desalination Research Center of Excellence (EDRC), and the Desert Research Center (DRC).

AUTHOR CONTRIBUTIONS

All authors contributed to the study conception and design. Material preparation, data collection, and analysis were performed by A.H.M.E.-A., R.A.H., F.A.M., S.O., and E.O. The first draft of the manuscript was written, revised, and previous versions of the manuscript were commented. All authors read and approved the final manuscript.'

FUNDING

This work was supported by Institutional Links grant, ID 527426826, under the Egypt-Newton-Mosharafa Fund partnership. The grant is funded by the UK Department for Business, Energy and Industrial Strategy and Science, Technology and Innovation Funding Authority (STIFA) – project NO. 42717 (An Integrated Smart System of Ultrafiltration, Photocatalysis, Thermal Desalination for Wastewater Treatment) and delivered by the British Council.

DATA AVAILABILITY STATEMENT

Data cannot be made publicly available; readers should contact the corresponding author for details.

CONFLICT OF INTEREST

The authors declare there is no conflict.

REFERENCES

Abu Salem, H. S., Khatita, A. A., Abdeen, M. M., Mohamed, E. A. & El Kammar, A. M. 2017 Geo-environmental evaluation of Wadi El Rayan Lakes, Egypt, using remote sensing and trace element techniques. *Arabian Journal of Geosciences* **10** (10), 224.

Akkoyunlu, A. & Akiner, M. E. 2012 Pollution evaluation in streams using water quality indices: a case study from Turkey's Sapanca Lake Basin'. *Ecological Indicators* **18**, 501–511.

Amini, H., Haghighat, G. A., Yunesian, M., Nabizadeh, R., Mahvi, A. H., Dehghani, M. H., Davani, R., Aminian, A.-R., Shamsipour, M. & Hassanzadeh, N. 2016 Spatial and temporal variability of fluoride oncentrations in groundwater resources of Larestan and Gerash regions in Iran from 2003 to 2010. *Environmental Geochemistry and Health* **38**, 25–37.

Appelo, C. A. J. & Postma, D. 1994 *Geochemistry Groundwater and Pollution*. AA Balkema, Rotterdam.
ASTM 2002 Water and Environmental Technology. *Annual Book of ASTM Standards,* Sec., 11: 11.01 and 11.02. American Society for Testing and Materials, West Conshohocken, NJ.
Atwa, A. F. M., Negm, A. & Armanuos, A. M. 2015 Environmental threats of an onsite sewage disposal on groundwater at Minia-Al Qamh, Sharkia Governorate, Egypt. In *Eighteenth International Water Technology Conference, IWTC18*, 12–14 March 2015, Sharm El Sheikh.
Berihu, B. A., Ugur, D. E. & Mehmet, C. 2017 Assessment of hydrogeochemistry and environmental isotopes of surface and groundwaters in the Kutahya Plain, Turkey. *Journal of African Earth Sciences* **134**, 230–240.
Boyacioglu, H. 2007 Surface water quality assessment by environmental methods. *Environmental Monitoring and Assessment* **131** (1–3), 371–376.
Cude, C. G. 2001 Oregon water quality index a tool for evaluating water quality management effectiveness'. *Journal of the American Water Resources Association* **37** (1), 125–137.
Davis, J. C. 1986 *Statistics and Data Analysis in Geology*. John Wiley and Sons, NY, Toronto-Singapore.
Deutsch, W. J. 1997 *Groundwater Geochemistry: Fundamentals and Applications to Contamination*. CRC Press, Boca Raton.
Drever, J. I. 1997 *The Geochemistry of Natural Waters: Surface and Groundwater Environments*. Prentice Hall, New Jersey.
El Alfy, M., Alharbi, T. & Mansour, B. 2018 Integrating geochemical investigations and geospatial assessment to understand the evolutionary process of hydrochemistry and groundwater quality in arid areas. *Environmental Monitoring and Assessment* **190**, 277. https://doi.org/10.1007/s10661-018-6640-4.
El-Sayed, S. A., Ezz El Din, M. R. & Deyab, M. E. 2011 Hydrogeological Investigations of the Quaternary Aquifer in the northern part of El-Sharkia Governorate, Egypt. *Isotope & Radiation Research* **43** (4), 1595–1619.
Embaby, A. A., Afifi, S. Y. & El Atabany, N. M. 2014 Hydrochemical evaluation of Belbies district groundwater, South El Sharkia Governorate, Egypt. *Life Science Journal* **11** (12s), 1074–1092. (ISSN: 10978135). Available from: http://www.lifesciencesite.com.
Fakhri, Y., Saha, N., Ghanbari, S., Rasouli, M., Miri, A. & Avazpour, M. 2018 Carcinogenic and non-carcinogenic health risks of metal (oid) s in tap water from Ilam city, Iran. *Food and Chemical Toxicology* **118**, 204–211.
Fishman, M. J. & Friedman, L. C. 1989 Methods for determination of inorganic substances in water and fluvial sediments. In *US Geological Survey Techniques of Water Resources Investigations*, Book 5, Chapter A1. USGS, Reston, VA.
Garrels, R. M. & MacKenzie, F. T. 1971 *Evolution of Sedimentary Rocks*. Norton, New York.
Gibbs, R. J. 1970 Mechanisms controlling world's water chemistry. *Science* **170**, 1088–1090.
Hair, J. F., Anderson, R. E., Tatham, R. & Black, W. C. 1992 *Multivariate Data Analysis with Readings*, 3rd edn. Macmillan Publishing Company, New York.
Kaiser, H. F. 1960 The application of electronic computers to factor analysis. *Educational and Psychological Measurement* **20**, 141–151.
Kamani, H., Mirzaei, N., Ghaderpoori, M., Bazrafshan, E., Rezaei, S. & Mahvi, A. H. 2018 Concentration and ecological risk of heavy metal in street dusts of Eslamshahr, Iran. *Human Ecology and Risk Assessment* **24**, 961–970.
Keramati, H., Ghorbani, R., Fakhri, Y., Khaneghah, A.M., Conti, G.O., Ferrante, M., Ghaderpoori, M., Taghavi, M., Baninameh, Z. & Bay, A. 2018a Radon 222 in drinking water resources of Iran: a systematic review, meta-analysis and probabilistic risk assessment (Monte Carlo simulation). *Food and Chemical Toxicology* **115**, 460–469.
Keramati, H., Miri, A., Baghaei, M., Rahimizadeh, A., Ghorbani, R., Fakhri, Y., Bay, A., Moradi, M., Bahmani, Z. & Ghaderpoori, M. 2018b Fluoride in Iranian drinking water resources: a systematic review, meta-analysis and non-carcinogenic risk assessment. *Biological Trace Element Research* **188** (2), 261–273.
Khan, K., Lu, K., Khan, H., Zakir, S., Ihsanullah, Khan, S., Khan, A. A., Wei, L. & Wang, T. 2013a Health risk associated with heavy metals in the drinking water of swat northern swat. *Journal of Environmental Sciences* **25**, 2003e13.
Khan, M. U., Malik, R. N. & Muhammad, S. 2013b Human health risk from heavy metal via food crops consumption with wastewater irrigation practices in Pakistan. *Chemosphere* **93**, 2230–2238.
Kusin, F. M., Azani, N. N. M., Hasan, S. N. M. S. & Sulong, N. A. 2018 Distribution of heavy metals and metalloid in surface sediments of heavily-mined area for bauxite ore in Pengerang, Malaysia and associated risk assessment. *Catena* **165**, 454e464.
Liu L., Zhang & Zhong, T., 2016 Pollution and health risk assessment of heavy metals in urban soil in China. *Human and Ecological Risk Assessment* **22**, 424–434.
Liu, F., Zhao, Z., Yang, L., Ma, Y., Xu, Y., Gong, L. & Liu, H. 2020 Geochemical characterization of shallow groundwater using statistical analysis and geochemical modeling in an irrigated region along the upper Yellow River, Northwestern China. *Journal of Geochemical Exploration* **215**, 106565.
Lloyd, J. W. & Heathcote, J. 1985 *Natural Inorganic Hydrochemistry in Relation to Groundwater*. Oxford University Press, New York.
Mabrouk, B., Ramadan, F., Nagaty, M. & Abd El Azeem, Y. 2016 Sedimentological and hydrogeochemical studies of the quaternary groundwater aquifer in El Salhyia Area, Sharkia Governorate, Egypt. *Middle East Journal of Applied Sciences* **6** (1), 120–138.
Mahgoub, S., Samaras, P., Abdel basit, H. & Abdelfattah, H. 2015 Seasonal variation in microbiological and physicochemical characteristics of municipal wastewater in Al-Sharqiya province, Egypt (case study). *Desalination and Water Treatment* **57** (5), 2355–2364.
Mansour, N. M. 2020 Hydrochemical studies and evaluation of groundwater quality of the aquifer at Faquss, Al Sharqia governorate, Egypt. *Sustainable Water Resources Management* **6**, 19. https://doi.org/10.1007/s40899.quaternary-020-00374-y.

Matiatos, I., Alexopoulos, A. & Godelitsas, A. 2014 Multivariate statistical analysis of the hydrogeochemical and isotopic composition of the groundwater resources in northeastern Peloponnesus (Greece). *Science of the Total Environment* **476–477**, 577–590. https://doi.org/10.1016/j.scitotenv.2014.01.042.

Moghaddama, A., Moteallemib, A., Joulaeic, F. & Peirovi, R. 2018 A spatial variation study of groundwater quality parameters in the Gonabad Plain using deterministic and geostatistical models. *Desalination and Water Treatment* **103**, 261–269.

Mohamed, I., Othman, F., Ibrahim, A. I. N., Alaa-Eldin, M. E. & Yunus, R. M. 2015 Assessment of water quality parameters using multivariate analysis for Klang River basin, Malaysia. *Environmental Monitoring and Assessment* **187**, 4182. https://doi.org/10.1007/s10661-014-4182-y.

Parkhurst, D. L. & Appelo, C. A. J. 1999 *User's Guide to PHREEQC (Version 2) A Computer Program for Speciation, Batch-Reaction, One Dimensional Transport, and Inverse Geochemical Calculations*. United States Geological Survey, Water Resources, Investigations Report 99-4259, Washington, DC, p. 326.

Piper, A. M. 1944 A graphic procedure in the geochemical interpretation of water analysis. *Transactions of the American Geophysical Union* **25**, 914–923.

Rainwater, F. H. & Thatcher, L. L. 1960 Methods for collection and analysis of water samples. *U.S. Geological Survey Water Supply Papers* **1454**, 1–301.

Rashed, H. S. A. 2016 Determination of soil productivity potentials: a case study in El-Sharkia Governorate of Egypt. *Egyptian Journal of Soil Science* **56** (4), 639–665.

Rezaei, H., Jafari, A., Kamarehie, B., Fakhri, Y., Ghaderpoury, A., Karami, M. A., Ghaderpoori, M., Shams, M., Bidarpoor, F. & Salimi, M. 2018 Health risk assessment related to the fluoride, nitrate, and nitrite in the drinking water in the Sanandaj, Kurdistan County, Iran. *Human Ecology and Risk Assessment* **25**, 1242–1250.

Shah, M. T., Ara, J., Muhammad, S., Khan, S. & Tariq, S. 2012 Health risk assessment via surface water and sub-surface water consumption in the mafic and ultramafic terrain Mohmand agency northern Pakistan. *Journal of Geochemical Exploration* **118**, 60e70.

Slimani, R., Guendouz, A., Trolard, F., Moulla, A. S., Hamdi-Aissa, B. & Bourrie, G. 2015 Geochemical inverse modeling of chemical and isotopic data from groundwaters in Sahara (Ouargla basin, Algeria). *Hydrology and Earth Systems Discussions*. https://doi.org/10.5194/hess-2015-385.

Sohrabi, Y., Saeidi, M., Biglari, H., Rahdar, S., Baneshi, M.M., Ahamadabadi, M., Narooie, M.R, Khaksefidi, R. & Alipour, V. 2016 Heavy metal concentrations in water resources of rural areas of Kermanshah. *Iranian IIOAB Journal* **7**, 542–546.

Sultana, M. S., Rana, S., Yamazaki, S., Aono, T. & Yoshida, S. 2017 Health risk assessment for carcinogenic and non-carcinogenic heavy metal exposures from vegetables and fruits of Bangladesh. *Cogent Environmental Science* **3**, 1291107.

Tani, F. & Barrington, S. 2005 Zinc and copper uptake by plants under two transpiration rates. part II. Buckwheat (Fagopyrum esculentum L.). *Environmental Pollution* **138**, 548–558.

Tepanosyan, G., Maghakyan, N., Sahakyan, L. & Saghatelyan, A. 2017 Heavy metals pollution levels and children health risk assessment of Yerevan kindergartens soils. *Ecotoxicology and Environmental Safety* **142**, 257–265.

TSE 1998 *Water Quality – Determination of Dissolved Anions by Liquid Chromatography of Ions – Part 1: Determination of Bromide, Chloride, Fluoride, Nitrate, Nitrite, Phosphate and Sulfate. Section 1: Method for Less Polluted Waters*. Turkish Standard Institution, Turkey.

USEPA 2005 *Guidelines for Carcinogen Risk Assessment. Risk Assessment Forum*. United States Environmental Protection Agency, Washington, DC. EPA/630/P-03/001F.

USEPA 2009 *National Primary Drinking Water Regulations*. EPA 816-F-09-004. United States Environmental Protection Agency, Washington DC.

USEPA 2012 *Integrated Risk Information System (IRIS) Electronic Database U.S. Edition of the Drinking Water Standards and Health Advisories. 2012 Ed Drink Water Stand Heal Advise*. https://doi.org/EPA822-S-12-001.

WHO 2004 *Guidelines for Drinking Water Quality*. Vol. 1, 3rd edn. World Health Organization, Geneva, Switzerland (ISBN 92 4 1546387).

WHO 2011 *Guidelines for Drinking-Water Quality*. 4th edn. World Health Organization, Geneva, Switzerland. Available from: http://apps.who.int/iris/bitstream/10665/44584/1/9789241548151_eng.pdf. (accessed 7 April 2016).

WHO 2017 *Guidelines for Drinking Water Quality [Electronic Resource]*. 4th edn. Geneva, pp. 307–441. (ISBN: 978 92 4 154815 1 (WEB version). Available from: http://whqlibdoc.who.int/publications/2011/9789241548151_eng.pdf.

Yousefi, M., Dehghani, M. H., Nasab, S. M., Taghavimanesh, V., Nazmara, S. & Mohammadi, A. A. 2018 Data on trend changes of drinking groundwater resources quality: a case study in Abhar. *Data Brief* **17**, 424–430.

Zhou, Y., Li, P., Peiyue, L., Chen, M., Dong, Z. & Lu, C. 2020 Groundwater quality for potable and irrigation uses and associated health risk in southern part of Gu'an County, North China Plain. *Environmental Geochemistry and Health* **43**, 813–835.

First received 27 November 2022; accepted in revised form 30 April 2023. Available online 15 May 2023